CINEFORUM
ISSN: 0009-7039
Vol. 66. No. S8, 2026 (Special Issue S8)

Design, Formulation and Evaluation of a mucoadhesive buccal film of mometasone furoate for allergic conditions

Anuja Sadashiv More[1*], Ms. Manisha Mane[2], Ms. Akshada Deshmukh[2], Mr. Rushikesh Kumbhar[1], Ms. Fatima Sheikh[1], Ms. Vaishnavi Koulge[3], Ms. Shradha Bhosale[1], Mr. Ashutosh Kamble[4]

[1]Student, Department of Pharmaceutics, Ashokrao Mane College of Pharmacy, Peth Vadgaon
[2]Assistant Professor, Department of Pharmaceutics, Ashokrao Mane College of Pharmacy, Peth Vadagaon
[3]Assistant Professor, Department of Pharmacology, D.Y. Patil College of Pharmacy, Kolhapur,
[4]D. Y. Patil Education Society (Deemed to be University), Kolhapur, Maharashtra State, India.
[5]Assistant Professor, Department of Pharmacognosy, D.Y. Patil College of Pharmacy, Kolhapur,
[6]D. Y. Patil Education Society (Deemed to be University), Kolhapur, Maharashtra State, India

***Corresponding Author**
Anuja Sadashiv More
1Student, Department of Pharmaceutics, Ashokrao Mane College of Pharmacy, Peth Vadgaon

ABSTRACT
Mometasone Furoate is a synthetic corticosteroid distinguished by its potent anti-inflammatory and anti-allergic action and low systemic side effects compared with other corticosteroids, making it a potential drug for local buccal delivery. The present study aimed to design a mucoadhesive buccal film containing fluticasone that is aesthetically acceptable and could maintain local drug release for a sustained period to manage the signs and symptoms of different allergic conditions. The solvent casting technique was used in film preparation. Different polymeric blends were used either alone or in combination with mucoadhesive polymers, sodium carboxymethyl cellulose (SCMC), or Carbopol 971P at different concentrations. The physicochemical properties, in vitro mucoadhesion time, as well as the drug release properties for all prepared formulations were determined. Selected formulations with adequate properties were further examined by differential scanning calorimetry (DSC) and X-ray diffraction (XRD) and subjected to in vivo evaluation. Films containing hydroxypropyl methylcellulose (HPMC)/ ethyl cellulose (EC) showed acceptable physicochemical properties, homogeneous drug distribution, convenient mucoadhesion time, moderate swelling, as well as sustained drug release up to 30min.

Keywords: Buccal Film, Drug Delivery System, Mometasone Furoate, corticosteroid, mucoadhesive, Allergic conditions

INTRODUCTION
Allergy illnesses are systemic issues brought on by a compromised or hyperactive immune system. A complicated interplay between genetic and environmental variables leads to the development of these diseases. Food allergies, eczema, atopic dermatitis, allergic rhinitis, and allergic asthma syndrome are examples of allergic disorders. According to the World Health Organisation, allergic disorders are among the top three medical conditions that need to be prevented and well managed in the twenty-first century.[(1-3)] Despite being a systemic ailment, allergic disease can cause a number of localised health issues and, in extreme situations, anaphylactic shock. The rising incidence of allergic illnesses has a significant impact on patients. In various populations, asthma-related death rates range from 90 to 170 per million, with low- and middle-income nations accounting for over 96% of these deaths. According to current estimates, 1–10% of people suffer from food allergies. The lifetime prevalence of atopic dermatitis is approximately 20%, and its global prevalence is close to 8%. Around 171.17 million people worldwide suffered from atopic dermatitis in 2019.[(4-8)] symptoms such as nasal congestion. Because eosinophils, mast cells, and T helper 2 cells infiltrate both allergic rhinitis.

Mucoadhesive Buccal Film:[(9-15)]
Muco-adhesive buccal films are the most current advancement in buccal administration. They are now more important than ever as patient-friendly, cost-effective, and cutting-edge Active Pharmaceutical Ingredient (API) delivery techniques. Muco-adhesive buccal films can be made to have both local and systemic activity because they are made to adhere to one another. Compared to buccal pills, the muco-adhesive buccal films might be more comfortable and flexible. Muco-adhesive buccal films deliver API straight into the bloodstream through the internal jugular vein, bypassing the liver's first-pass processing. The large surface area of the mucoadhesive buccal film facilitates rapid moistening, accelerating the absorption of the API. Due to its abundant blood supply, the buccal mucosa is a crucial area for medication absorption. Since the dosage form is easy to provide to paediatric and

OPEN ACCESS © CINEFORUM

elderly patients, as well as those who are mentally challenged, uncooperative, or have physical or mental problems, its bioavailability is boosted by extending its residence time at the site of absorption.

1.2 Anatomy and physiology of oral mucosa[16-26]

Because the oral mucosa is lubricated and sticky, there is less friction as cells move relative to one another. The buccal cavity, lingual area, palate, and gingival region are the four locations where drugs have been administered. Of the four locations listed above, the buccal route is the most often used site Cosa of the buccal and sublingual regions is more permeable because it contains very little ceramide.

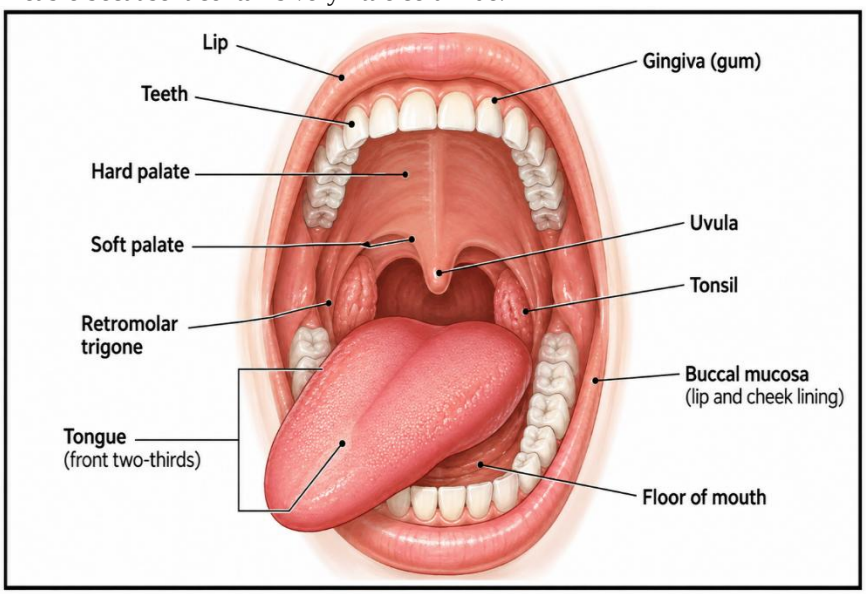

Fig. No. 1 Oral Cavity

1.3 Mechanism of Buccal Absorption:[27-30]

Better drug absorption occurs when non-isolated or individual species disperse slowly. Through entangled epithelial gaps, the concentration gradient contributes significantly to the regulation of the entire process. The main mode of transport is the movement of non-ionic species over the buccal lipid membrane. Like many other mucosal pores, the buccal mucosa is thought to be a lipoidal barrier to drug overdose since it is where the drug molecule is most readily absorbed when it is lipophilic. The initial dosage protocol provides a sufficient explanation for the dynamics of buccal medication absorption. Tomlinson and Dearden (1971) have demonstrated that saliva starts to modify the buccal absorption kinetics from a pharmacological solution by significantly altering the drug excess in the mouth. The following is the relationship between saliva and time:

$$\frac{dm}{dt} = \frac{Kc}{ViVt}$$

Where, M - Mass of drug in the mouth at time t K - Proportionality constant
C - Concentration of drug in the mouth at time
Vi - The volume of solution in the mouth cavity and Vt - Salivary secretion rate

1.4 Manufacturing Methods[31]

The buccal film manufacturing process includes the following techniques Solvent casting technique
Hot melt extrusion technique Direct Milling
Solid dispersion extrusion Semisolid casting

OPEN ACCESS © CINEFORUM

Sr. No.	Materials Used	Name of supplier
1	HPMC E 15	LOBA Chemicals
2	Polyethene glycol 400	LOBA Chemicals
3	Citric Acid	LOBA Chemicals
4	Polyvinyl Propylene	LOBA Chemicals
5	Sucralose	Bliss of Earth
6	Menthol	LOBA Chemicals
7	Ethanol	LOBA Chemicals
8	Distilled Water	-

Table No 1 - Materials Used and their Suppliers

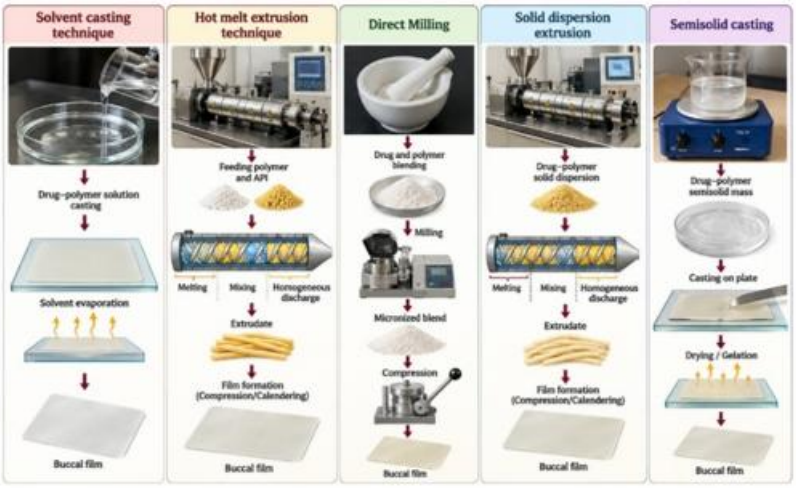

Fig No 2 Methods of preparation of buccal film

Materials

3.EXPERIMENTAL WORK[32-35]

3.1 Fourier Transform Infrared (FTIR) Analysis

FTIR analysis of pure Mometasone furoate and drug–excipient mixtures was performed over 4000–400 cm^{-1} to identify functional groups and assess compatibility. The drug's characteristic peaks remained without significant shifts or disappearance, indicating no major chemical interactions with the excipients and confirming their suitability for formulation.

3.2 Drug Excipients Compatibility Study

Drug–excipient compatibility was assessed using an Agilent Cary 630 FTIR spectrophotometer over 4000–400 cm^{-1}. Drug, polymer, and excipients (1:1:1) were stored at 40°C/75% RH for one month, after which FTIR spectra showed no significant changes in the characteristic peaks of Mometasone furoate, indicating compatibility.

3.3 X-ray diffraction (XRD) Study

X-ray diffraction (XRD) was performed to evaluate the crystalline nature of Mometasone furoate and its physical form after formulation. The pure drug showed distinct crystalline peaks, while the drug–excipient mixture showed reduced peak intensity without new peaks, indicating retention of crystallinity and the absence of significant interaction.

3.4 Differential Scanning Calorimetry (DSC) study

DSC analysis was performed to study the thermal behaviour and drug–excipient compatibility of Mometasone furoate. The pure drug showed a characteristic endothermic peak, while the drug–excipient mixture showed no new peaks, indicating good compatibility and retention of the drug's crystalline nature.

3.5 Surface Electron Morphology (SEM) study

OPEN ACCESS © CINEFORUM

SEM was used to evaluate the surface morphology and particle characteristics of Mometasone furoate. The pure drug showed irregular crystalline particles with a rough surface, while the formulated system exhibited a smoother and more uniform surface, indicating proper drug dispersion within the excipients.

3.6 Formulation by 3^2 Full Factorial Design

Table No 2 Formulation Table for all 9 Batches Using 3^2 Full Factorial Design

Ingredients	F1	F2	F3	F4	F5	F6	F7	F8	F9
Mometasone Furoate	5	5	5	5	5	5	5	5	5
HPMC(mg)	200	300	400	200	300	400	200	300	400
PEG400(mg)	20	30	40	40	30	20	30	20	40
PVP(ml)	0.5	0.5	0.5	0.5	0.5	0.5	0.5	0.5	0.5
Ethanol(ml)	5	5	5	5	5	5	5	5	5
Sucralose(mg)	Q.S.	Q.S.	Q.S.	Q.S.	Q.S.	Q.S.	Q.S.	Q.S.	Q.S.
Distilled Water (ml)	20	20	20	20	20	20	20	20	20

3.7 Compositions and Responses of Factorial Design

Table No 3 Compositions and Responses of Factorial Design

Run	Factor 1	Factor 2	Response 1	Response 2
	A: HPMC E-15 (mg)	B: PEG 400 (mg)	Folding Endurance (No of times)	% Drug Release (min)
F1	200	20	132	95
F2	200	30	158	91
F3	200	40	184	93
F4	300	20	176	90
F5	300	30	214	88
F6	300	40	238	85
F7	400	20	229	82:
F8	400	30	256	79
F9	400	40	284	75

3.8 Formulation of Optimised Batch

Table N0 4 Formulation Table: Optimised Batch MBF

Sr. No	Name of Ingredients	Quantity Taken
1	Mometasone Furoate	5mg
2	HPMC E-15	300mg
3	PEG-400	30mg
4	PVP	0.5ml
5	Sucralose	q.s.
6	Ethanol	5ml
7	Distilled Water	q.s.

3.9 Evaluation of Mucoadhesive Buccal Film[36-50]

3.9.1 Physical Appearance

OPEN ACCESS © CINEFORUM

The prepared buccal films were visually examined for colour, clarity, smoothness, flexibility, cracks, air bubbles, and other visible defects. A uniform, smooth, and defect-free film was considered desirable.

3.9.2 Thickness
The thickness of the films was measured at different points using a digital micrometre or thickness gauge. The mean thickness was calculated to determine the uniformity of the film.
Formula:
Mean thickness = Σ thickness of individual measurements / Number of measurements

3.9.3 Weight Uniformity
Individual films of the same dimensions were accurately weighed using a digital balance. The average weight and percentage deviation were calculated to assess weight uniformity.
Formula:
Mean weight = Total weight of films / Number of films
% Deviation = (Individual weight − Mean weight) / Mean weight × 100

3.9.4 Folding Endurance
Folding endurance was determined by repeatedly folding the film at the same position until it broke. The number of folds required to break the film was recorded as its folding endurance.
Folding endurance = Number of folds before breaking

3.9.5 Surface pH
The surface pH of the buccal film was determined after moistening the film with a small quantity of distilled water. The pH was measured using a calibrated pH meter to assess the possibility of mucosal irritation.

3.9.6 Moisture Content
The moisture content of the film was determined by weighing the film before and after drying under specified conditions. It indicates the amount of moisture present in the formulation.
Formula:
% Moisture content = (Initial weight − Final weight) / Initial weight

3.9.7 Tensile Strength
Tensile strength represents the maximum stress that the film can withstand before breaking. It was determined using a suitable tensile testing instrument.
Formula:
Tensile strength = Breaking force / Cross-sectional area

3.9.8 Percent Elongation
Percentage elongation indicates the ability of the film to stretch before breaking. The initial and final lengths of the film were recorded during the tensile strength test.
Formula:
% Elongation = (Final length − Initial length) / Initial length × 100

3.9.9 Drug Content Uniformity
A specified quantity of the film was dissolved in a suitable solvent and analysed using an appropriate analytical method. The drug content was calculated to determine the uniform distribution of drug within the films.
Formula:
% Drug content = (Estimated drug content / Theoretical drug content) × 100

3.9.10 *In-Vitro* Mucoadhesion Strength Study
The mucoadhesive strength of the buccal film was determined by measuring the force required to detach the film from a suitable mucosal membrane. It indicates the ability of the film to adhere to the buccal mucosa.
Formula:
Mucoadhesive strength = Detachment force / Surface area of film

3.9. 11 *In-Vitro* Mucoadhesion Residence Time
The film was placed on a suitable mucosal membrane and maintained under conditions simulating the buccal environment. The time required for complete detachment or erosion of the film was recorded as the mucoadhesive residence time.

OPEN ACCESS © CINEFORUM

Mucoadhesive residence time = Time required for complete detachment/erosion

3.9.12 *In-Vitro* Permeation Study

Drug permeation through a suitable biological or synthetic membrane was studied using a diffusion cell, such as a Franz diffusion cell. Samples were withdrawn at predetermined intervals and analysed to determine the amount of drug permeated.
Formula:
Cumulative amount permeated = Amount of drug permeated per unit area of membrane
Flux (J) = dQ / (A × dt)
Where, Q = amount of drug permeated, A = diffusion area, and dt = time interval.

3.9.13. *In Vitro* Disintegration Study

The buccal film was placed in a suitable medium, and the time required for it to break down completely was recorded. A suitable disintegration apparatus may be used according to the experimental method.
Disintegration time = Time required for complete breakdown of the film

3.9.14 *In-Vitro* Drug Release Study

The film was placed in a suitable dissolution medium, and samples were withdrawn at predetermined time intervals. The samples were analysed to determine the percentage of drug released and the drug-release profile of the formulation.
Formula:
% Drug release = (Amount of drug released / Total amount of drug in film) × 100

3.9.15 Anti-Allergic Activity

The anti-allergic activity of the optimised buccal film was evaluated using an appropriate in-vitro biological model. The response of the formulation was compared with the control and standard to determine its anti-allergic potential.
% Inhibition = (Control response − Sample response) / Control response × 100

3.9.16 Accelerated Stability Study

The optimised buccal film was stored under accelerated stability conditions of specified temperature and relative humidity for a predetermined period. At selected intervals, the films were evaluated for appearance, drug content, and other critical parameters to determine their stability.
% Drug retained = (Drug content after storage / Initial drug content) × 100
% Drug loss = 100 − % Drug retained

4.RESULTS AND DISCUSSION

FTIR Spectra

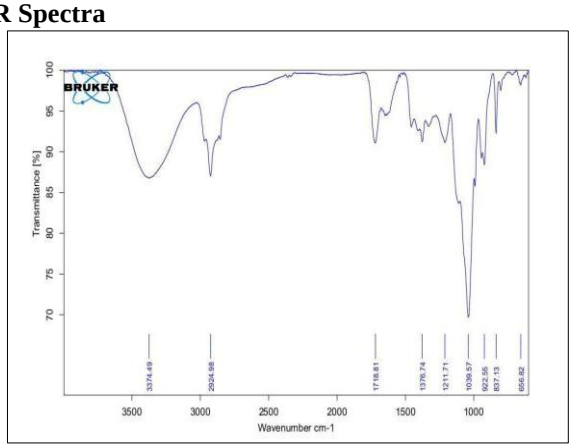

a

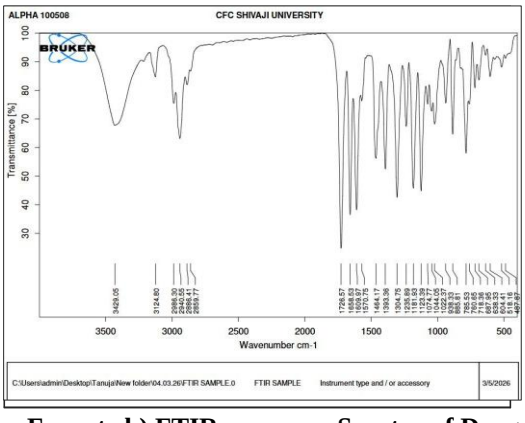

b

Fig. No. – 13 a) FTIR Spectra of Mometasone Furoate b) FTIR Spectra of Drug and excipients

OPEN ACCESS © CINEFORUM

Table No 5 Major Observed Peaks of Mometasone Furoate

Functional Groups	**Type**	**Standard wavenumber -1 range (cm)**	**Observed wavenumber range -1 (cm)**
O-H Stretching alcohol/phenol	Alcohol or Phenol	3200-3600	3429
C-H Stretching aromatic	Aromatic ring	3000-3100	3125
C=O Stretching carbonyl	Ketone or conjugated Carbonyl	1680-1750	1703
C=C Stretching Aromatic	Aromatic ring or alkene	1450-1600	1606
NO_2 Stretching Aromatic	Aromatic ring	1500-1600	1571
CH_2/CH3 Stretching ethyl methyl	Methyl	1450-1470	1461
C-N Stretching Amine	Amine	1250-1360	1303
C-O-C Stretching Ether	Ether	1050-1275	1169
C-F/C-Cl Stretching Fluro or chloro	Fluro or chloro group	1000-1400	1044
C-H bending (out of plane bonding)	Aromatic ring	900-1000	963

Differential Scanning Calorimetry (DSC) study

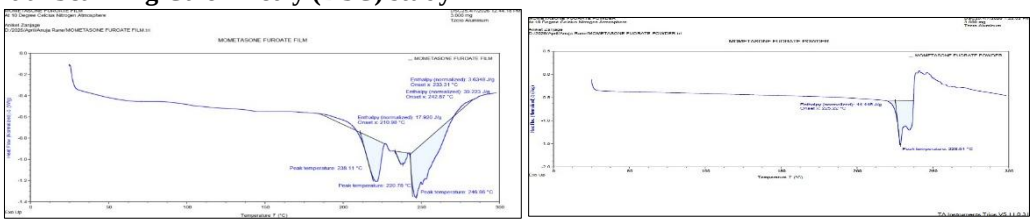

Fig No. a) Differential Scanning Calorimetry of mometasone furoate b)Differential Scanning Calorimetry of drug and mometasone furoate mixture

X-ray diffraction study

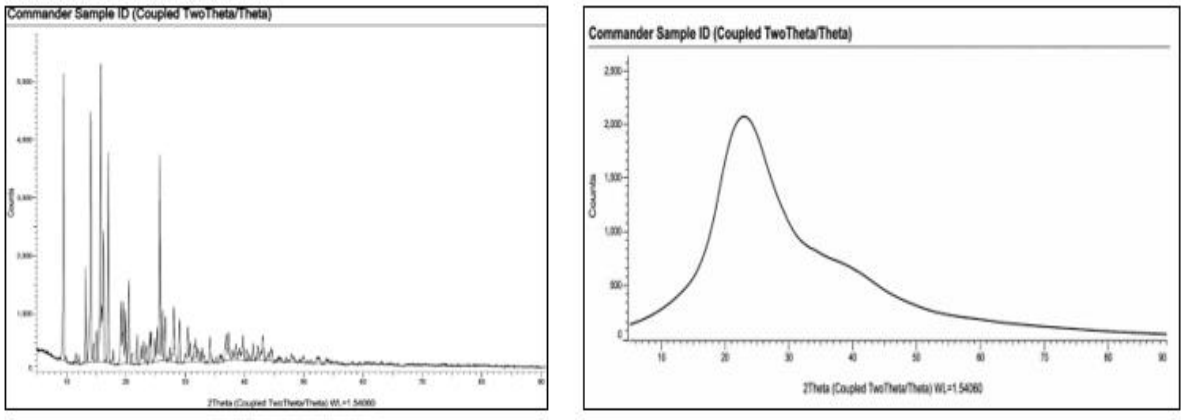

Fig No 15 X-ray diffraction study of mometasone furoate b) X-ray diffraction study of drug and excipients

4.4 Formulation by 3^2 Full Factorial Design

A 3^2 factorial design was used to optimize the buccal films, with HPMC and PEG 400 concentrations selected as independent variables. Each variable was studied at three levels (−1, 0, +1), resulting in 9 experimental formulations.

OPEN ACCESS © CINEFORUM

3^2 Full Factorial Design for MBF

Table No 6 3^2 Full Factorial Design for MBF

Factors	**Polymer(mg)**			**Plasticizer (mg)**		
Concentration	200	300	400	2	3	4
Level	0	-1	+1	0	-1	+1

Table No 7 Formulation Table for all 9 Batches Using 3^2 Full Factorial Design

Ingredients	**F1**	**F2**	**F3**	**F4**	**F5**	**F6**	**F7**	**F8**	**F9**
Mometasone Furoate	5	5	5	5	5	5	5	5	5
HPMC(mg)	200	300	400	200	300	400	200	300	400
PEG400(mg)	20	30	40	40	30	20	30	20	40
PVP(ml)	0.5	0.5	0.5	0.5	0.5	0.5	0.5	0.5	0.5
Ethanol(ml)	5	5	5	5	5	5	5	5	5
Sucralose(mg)	Q.S.	Q.S.	Q.S.	Q.S.	Q.S.	Q.S.	Q.S.	Q.S.	Q.S.
Distilled Water (ml)	20	20	20	20	20	20	20	20	20

4.5 Compositions and Responses of Factorial Design

Table No 8 Compositions and Responses of Factorial Design

Run	**Factor 1**	**Factor 2**	**Response 1**	**Response 2**
	A: HPMC E-15 (mg)	**B: PEG 400 (mg)**	**Folding Endurance (No of times)**	**% Drug Release (min)**
F1	200	20	132	95
F2	200	30	158	91
F3	200	40	184	93
F4	300	20	176	90
F5	300	30	214	88
F6	300	40	238	85
F7	400	20	229	82
F8	400	30	256	79
F9	400	40	284	75

4.6 ANOVA for Linear Model

Table No 9 : Response 1: Folding Endurance

Source	**Sum of Squares**		**df**	**Mean Square**	**F-value**	**P-value**	
Model	39327.80		2	19663.90	5.32	0.0468	**Significant**
A-HPMC	32474.98		1	32474.98	8.79	0.0251	
B-PEG 400	6852.82		1	6852.82	1.86	0.221	
	22161.09		6	3693.52			
	61488.89		8				

Table. No 10: Fit Statics

Source	**Sequential p-value**	**Lack of Fit p-value**	**Adjusted R^2**	**Predicted R^2**	
Linear	**0.0468**		**0.5195**	**0.2437**	**Suggested**
2Fl	0.2870		0.5508	0.1329	
Quadratic	0.3913		0.5995		
Cubic	0.1840		0.9593		
					Aliased

OPEN ACCESS © CINEFORUM

Final Equation in Terms of Coded Factors

Table. No 11: Final Equation in Terms of Coded Factors

Folding Endurance	**=**
+268.89	
+63.71	**A**
+29.27	**B**

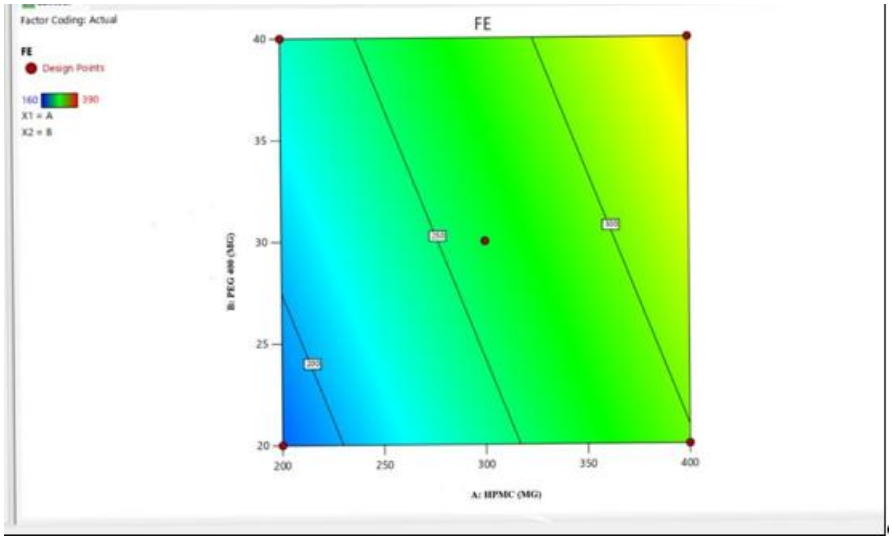

Fig.No. 3 :Counter Plot of Folding Endurance

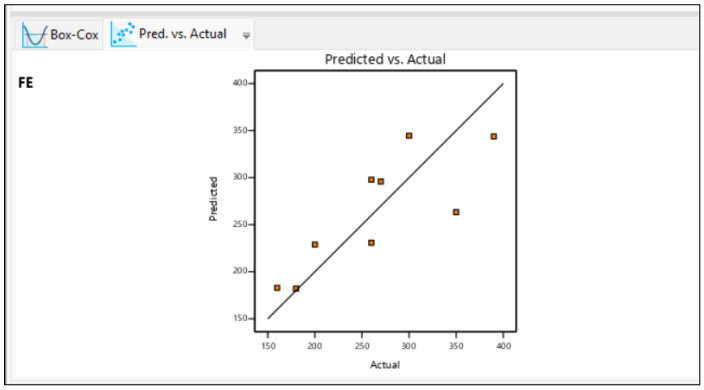

Fig. NO. 4 : The Predicted vs actual plot for folding endurance

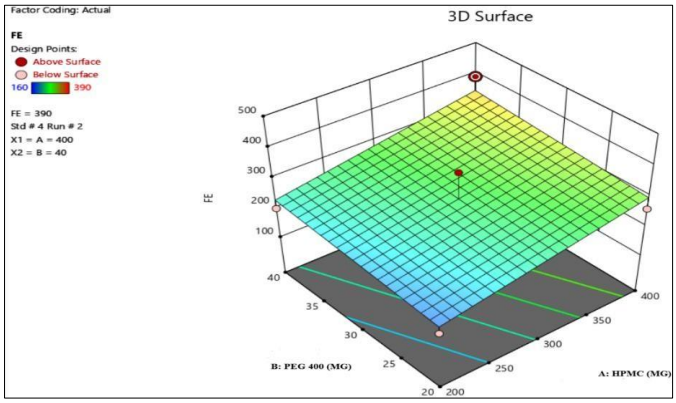

Fig No 5: 3D Surface Graph of Folding Endurance

OPEN ACCESS © CINEFORUM

ANOVA for Linear Model

Table. No 12: Response 2: % Drug Release

Source	Sum of squares	df	Mean Square	F-value	p-value	
Model	260.78	2	130.39	5.72	0.0407	significant
A-HPMC	159.56	1	159.56	7.00	0.0383	
B-PEG 400	101.22	1	101.22	4.44	0.0797	
Residual	136.78	6				
Cor total	397.56	8				

Table No. 13: Fit Statics

Source	Sequential p-value	Lack of Fit p-value	Adjusted R^2	Predicted R^2	
Linear	0.0407		0.5413	0.1718	Suggested
2Fl	0.1952		0.6196	-0.0646	
Quadratic	0.9093		0.4049		
Cubic	0.3754		0.7485		Aliased

Final Equation in Terms of Coded Factors

Table No 14: Final Equation in Terms of Coded Factors

Drug Release	=
+80.22	
-4.47	A
-3.56	B

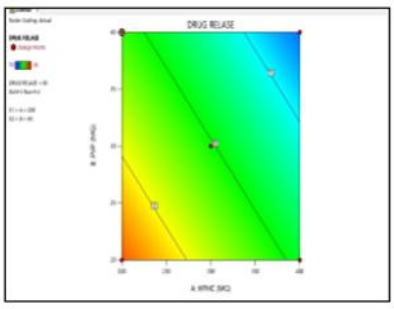

Fig No 6 : Plot of % Drug Release

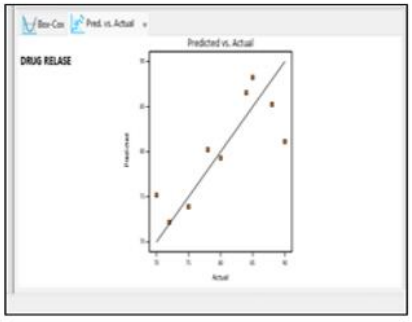

Fig No 7 : The predicted vs actual plot for % drug release

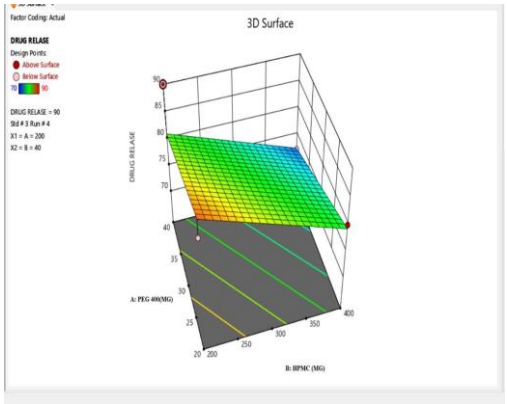

Fig No 8 : 3D surface graph of % drug release

OPEN ACCESS © CINEFORUM

4.10 Formulation of Optimized Batch as per Factorial Design

Table No 15 Formulation of Optimized Batch as per Factorial Design

Sr. No	Name of Ingredients	Quantity Taken
1	Mometasone Furoate	5mg
2	HPMC E-15	300mg
3	PEG-400	30mg
4	PVP	0.5ml
5	Sucralose	q.s.
6	Ethanol	5ml
7	Distilled Water	q.s.

4.11 Evaluation of Mucoadhesive Buccal Film

4.11.1 Physical Appearance

The physical appearance of the anti-allergic buccal film was simply checked by visual inspection and was found to be excellent.

4.11.2 Thickness

The thickness of all films was measured using a vernier calliper. The readings were taken at different positions and readings were taken in triplicate (n=3). The thickness of optimised batch F5 was found to be in an excellent range among all batches. The thickness of the optimised batch F5 was found to be 0.293mm.

4.11.3 Weight Uniformity

The weight uniformity was determined using a digital balance. This test is performed by using all 9 batches. The readings were taken in triplicate (n=3). The average of the three readings was calculated. The optimised batch F5 showed excellent weight uniformity in ideal range.

4.11.4 Folding Endurance

Folding endurance was measured manually. The point at which films get broken on folding at the same points. To check the folding endurance, all batches in triplicate (n=3) were measured. The average of three readings was calculated. The optimised batch F5 shows excellent results.

4.11.5 Surface pH

The surface pH was determined using a digital pH meter. The readings were taken in triplicate (n=3) for all batches. The pH of optimised batch F5 was found to be 6.8.

4.11.6 Moisture Content

The moisture content of all films is measured using a digital weighing balance. The readings of all 9 batches were taken in triplicate (n=3). The Moisture content of optimised batch F5 was found to be 3.93

4.11.7 Tensile Strength

The tensile strength results indicate the strength of the film and the risk of film cracking. However, no sign of cracking in the prepared mucoadhesive films was observed, which might be attributed to the addition of the plasticiser, PEG 400. Plasticisers are generally used to improve the mechanical properties of a polymer matrix. The tensile strength of the film was found to be between 12.80-51N/mm^2. The tensile strength of formulation F5% was found 51.00N/mm^2.

4.11.8 Percent Elongation

As manually force was applied to formulate an anti-allergic mucoadhesive buccal film. The final length that is the length increased after stretching and before the breaking of film was measured, and calculated percent elongation was found to be 32.50%.

4.11.9 Drug Content Uniformity

The % drug content uniformity is done to all 9 batches. The results of content uniformity indicated that the drug was uniformly dispersed. The drug content uniformity of the optimised mucoadhesive buccal film F5 was found to be 92.75%.

OPEN ACCESS © CINEFORUM

4.11.10 *In-Vitro* Mucoadhesion Strength Study
Mucoadhesion is a very important aspect for maintaining high drug levels at the site of administration and prevents expulsion of the formulation. The mucoadhesion strength of optimised batch F5 was found to be 27.3g.

4.11.11 *In-Vitro* Mucoadhesion residence time
The *In-vitro* mucoadhesion residence time of optimised batch F5 was found to be 25min.

4.11.12 *In vitro* Permeation Study
The *In-Vitro* Permeation of optimised batch F5 was found to be 83.47

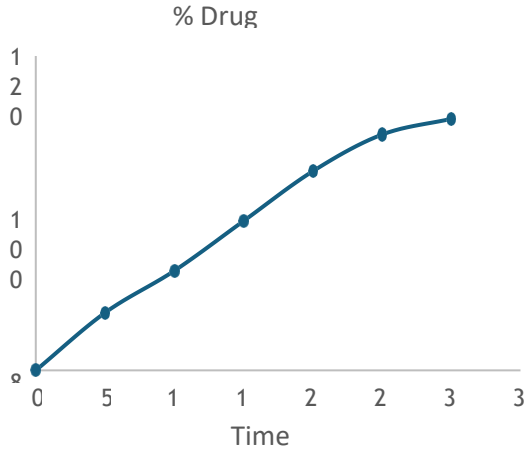

% Drug Permeation of optimised batch F5

4.11.13 *In vitro disintegration* study
The *in vitro* disintegration time of optimised film F5 was found to be 3min.

4.11.14 *In vitro* Drug Release
The *In-Vitro* drug release of optimised batch F5 was found to be 96.18%.

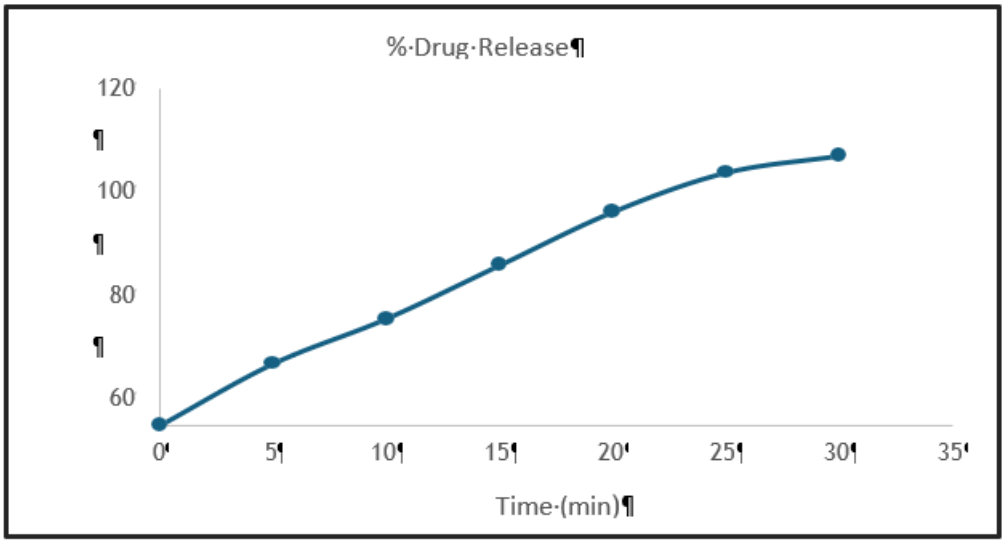

4.11.16 Anti-Allergic Activity Study
The anti-allergic activity of MF-01 was evaluated using an IgE-mediated RBL-2H3 mast cell degranulation assay. MF-01 showed concentration-dependent inhibition of β-hexosaminidase release, with 62.04% inhibition at 100 µg/mL, compared with 69.03% for dexamethasone, indicating significant anti-allergic potential.

OPEN ACCESS © CINEFORUM

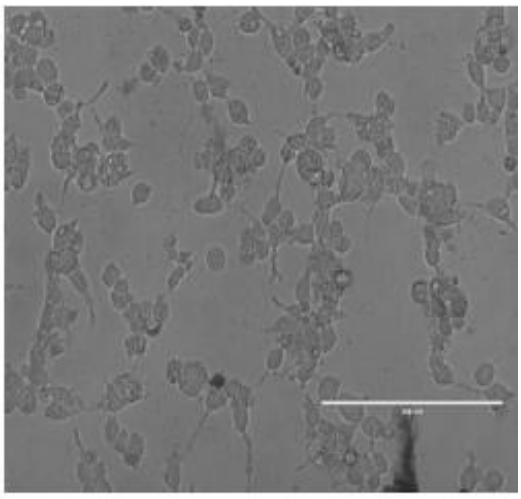

Control of test

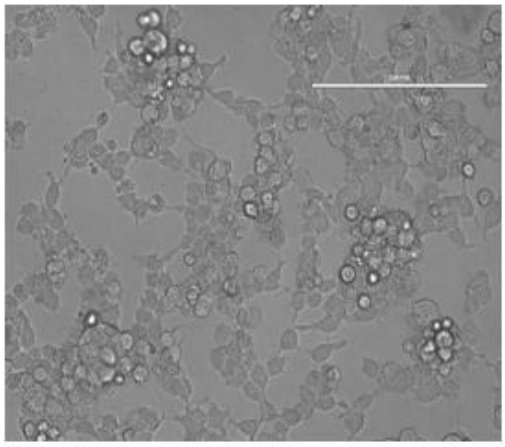

Film used test

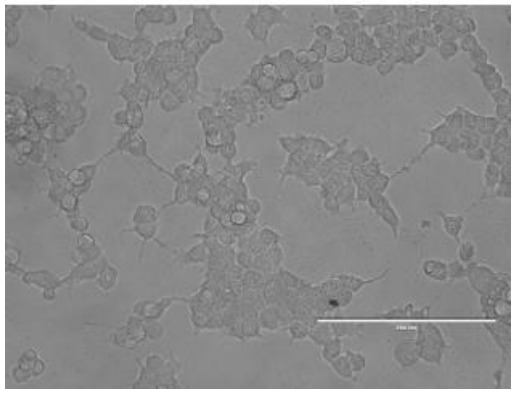

STD for test

Degranulation Assay

OPEN ACCESS © CINEFORUM

SR NO	SAMPLE CODE	Concentrations (µg/mL)	OD at 550 nm			Mean	% of Inhibition
1	Induced Control (IgE + Antigen)	-	-			0.988	-
2	Standard (Dexamethasone)	**20**	0.739	0.742	0.745	**0.742**	**24.90%**
		40	0.611	0.614	0.617	**0.614**	**37.85%**
		60	0.498	0.502	0.503	**0.501**	**49.29%**
		80	0.392	0.398	0.395	**0.395**	**60.02%**
		100	0.303	0.307	0.308	**0.306**	**69.03%**
3	**MF-01**	**20**	0.814	0.815	0.819	**0.816**	**17.41%**
		40	0.701	0.704	0.707	**0.704**	**28.74%**
		60	0.586	0.588	0.563	**0.579**	**41.40%**
		80	0.468	0.472	0.47	**0.47**	**52.43%**
		100	0.372	0.378	0.375	**0.375**	**62.04%**

Table no. 16 Anti-Allergic activity using IgE-Mediated RBL-2CH3 Mast Cell

Graphical Data:

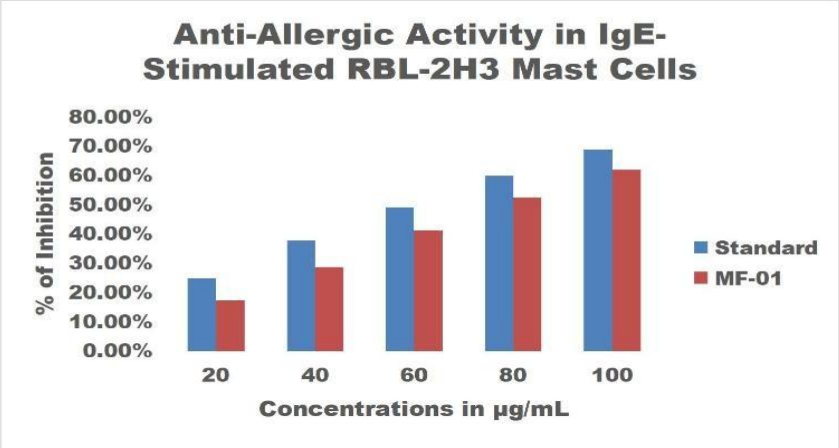

Graphical data of anti-allergic activity in IgE-stimulated RBL-2 mast cells

4.11.17 Accelerated Stability Study

The optimised batch F5 was evaluated for the stability study. Surface pH, disintegration time, and folding endurance are the parameters used for the stability study of the optimised batch.

Table No 17 Accelerated Stability Study of optimized batch F5

Parameters	Initial	After 1 month	After 2 month	After 3 month
Surface pH	6.8	6.3	6.2	6
Disintegration time(min)	3	4	6	7
Folding Endurance	214	210	207	204

Statement Declaration

Funding: The authors declare that no funds, grants or other support were received during the preparation of this manuscript.

Competing Interest: The authors have no relevant financial or non-financial interests to disclose.

Author Contribution: Conceptualizaton, investigation, formal analysis.

Data Availability: The datasets generated and analyzed during the current study are available form the corresponding author on reasonable request.

OPEN ACCESS © CINEFORUM

Ethics Approval: This study did not involve human participants or live animals. Goat skin was obtained as a slaughterhouse by-product. The RBL-2CH3 mast cell was obtained from source and authentication.
Consent to participate and to publish: Not applicable
Use of AI tools: An AI assistant was used to restructure the manuscript to the journal's guidelines and to edit the language of text written by the authors. The authors checked all content, data and references and take full responsibility for the manuscript.

REFERENCES

1. Wang J, Zhou Y, Zhang H, Hu L, Liu J, Wang L, et al. Pathogenesis of allergic diseases and implications for therapeutic interventions. Signal Transduction and Targeted Therapy. 2023;8(1):138.134-144.
2. Meghji, J., Mortimer, K., Jayasooriya, S. & Marks, G. B. Lung health in LMICs: tackling challenges ahead – Authors' reply. Lancet 398-490 (2021).
3. Tsoi LC, Rodriguez E, Degenhardt F, Baurecht H, Wehkamp U, Volks N, et al. Progression of acute-to-chronic atopic dermatitis is associated with quantitative rather than qualitative changes in cytokine responses. Journal of Allergy and Clinical Immunology. 2020;145(5):1406-1415
4. Lloyd-Lavery A, Rogers NK, Abuabara K, et al. What's new in atopic eczema? An analysis of systematic reviews published in 2016. Part 2: epidemiology, aetiology and risk factors. Clinical and Experimental Dermatology. 2019;44(4):370-375.
5. Dong WL, Ghosh R, Guo C, et al. The prevalence and years lived with disability of atopic dermatitis in China: findings from the Global Burden of Disease Study 2019. World Allergy Organisation Journal. 2021;14(11):100-118
6. Agache I, Miller R, Gern JE, Hellings PW, Jutel M, Muraro A, et al. Emerging concepts and challenges in implementing the exposome paradigm in allergic diseases and asthma: a PRACTALL document. Allergy. 2019;74(3):449-463
7. Demirdag Y, Bahna SL. The role of genetics in food allergy. Expert Review of Clinical Immunology. 2022;18(4):401-411
8. Choi BY, Han M, Kwak JW, Kim TH. Genetics and epigenetics in allergic rhinitis. Genes. 2021;12(12):201-215
9. Wu X, et al. Aberrant expressions of circulating lncRNA NEAT1 and microRNA-125a are linked with Th2 cells and symptom severity in pediatric allergic rhinitis. Journal of Clinical Laboratory Analysis. 2022;36(6): 136-148
10. Wen CL, Sundaram GM, Shan Q, Guang LG, Sampath P. Belinostat resolves skin barrier defects in atopic dermatitis by targeting the dysregulated miR-335:SOX6 axis. Journal of Allergy and Clinical Immunology. 2020;146(3):606-620.
11. Zhou B, et al. Notch signaling pathway: architecture, disease, and therapeutics. Signal Transduction and Targeted Therapy. 2022;7(1):95-108
12. Tindemans I, et al. Increased surface expression of NOTCH on memory T cells in peripheral blood from patients with asthma. Journal of Allergy and Clinical Immunology. 2019;143(2):769-771
13. Hammad H, Lambrecht BN. Wnt and Hippo pathways in regulatory T cells: a NOTCH above in asthma. Nature Immunology. 2020;21(11):1313-1314.
14. Jiao WE, et al. Notch signaling promotes development of allergic rhinitis by suppressing Foxp3 expression and Treg cell differentiation. International Archives of Allergy and Immunology. 2019;178(1):33-44.
15. Jiang S, Han S, Chen J, Li X, Che H. Inhibition effect of blunting Notch signaling on food allergy through improving TH1/TH2 balance in mice. Ann Allergy Asthma Immunol. 2017;118(1):94–102
16. Dell'Aringa M, Reinhardt RL. Notch signaling represents an important checkpoint between follicular T-helper and canonical T-helper 2 cell fate. Mucosal Immunol. 2018;11(4):1079–1091
17. Marenholz I, et al. Genome-wide association study identifies the SERPINB gene cluster as a susceptibility locus for food allergy. Nat Commun. 2017;8:1056-1062
18. Waage J, et al. Genome-wide association and HLA fine-mapping studies identify risk loci and genetic pathways underlying allergic rhinitis. Nat Genet. 2018;50(8):1072–1080
19. Ang H, Kim M, Hong JY, Cho HJ, Kim KW. Mitochondrial and nuclear mitochondrial variants in allergic diseases. Allergy Asthma Immunol Res. 2020;122-125
20. Qian L, Mehrabi NE, Athari SM, Athari SS. Mitochondria signaling pathways in allergic asthma. J Investig Med. 2022;70:863–882
21. Xu CJ, Gruzieva O, Qi C, Esplugues A, Koppelman GH. Shared DNA methylation signatures in childhood allergy: the MeDALL study. J Allergy Clin Immunol. 2020. 451-455
22. Schmidt AD, Strong CDG. Current understanding of epigenetics in atopic dermatitis. Exp Dermatol. 2021;30-42

OPEN ACCESS © CINEFORUM

23. Moussette S, Tuwaijri AA, Kohan-Ghadr HR, Elzein S, Naumova AK. Role of DNA methylation in expression control of the IKZF3-GSDMA region in human epithelial cells. PLoS One. 2017. 214-221
24. Yang IV, et al. The nasal methylome and childhood atopic asthma. J Allergy Clin Immunol. 2017.140-152
25. Alashkar Alhamwe B, et al. Decreased histone acetylation levels at Th1 and regulatory loci after induction of food allergy. Nutrients. 2020;121-135
26. Karam RA, Elrahman DA. Differential expression of miR-155 and Let-7a in the plasma of childhood asthma: potential biomarkers for diagnosis and severity. Clin Biochem. 2019.456-460
27. Tian M, et al. Changes in circulating microRNA-126 levels are associated with immune imbalance in children with acute asthma. Int J Immunopathol Pharmacol. 2018,32-45
28. Ye L, Yan M, Jian W, Jin ML. Effects of microRNA-19b on airway remodelling, airway inflammation and degree of oxidative stress by targeting TSLP through the Stat3 signalling pathway in a mouse model of asthma. Oncotarget. 2017;8:47533–47546.
29. Jin J, Feng X, Zhang J. Circular RNA circHIPK3 modulates the proliferation of airway smooth muscle cells by miR-326/STIM1 axis. Life Sci. 2020;255-260.
30. Shi J et al. miR-142-5p and miR-130a-3p regulate pulmonary macrophage polarisation and asthma airway remodelling. Immunol Cell Biol. 2020;98-108
31. Yan Z, et al. Decreased epithelial and sputum miR-221-3p associates with airway eosinophilic inflammation and CXCL17 expression in asthma. Am J Physiol Lung Cell Mol Physiol. 2018;315-324
32. Neidhart M. DNA methylation and complex human disease. Oxford: Academic Press; 2016 120-121
33. Xu CJ, Gruzieva O, Qi C, Esplugues A, Koppelman GH. Shared DNA methylation signatures in childhood allergy: the MeDALL study. J Allergy Clin Immunol. 2020 210-215
34. Boorgula MP, et al. Replicated methylation changes associated with eczema herpeticum and allergic response. Clin Epigenetics. 2019;11-22
35. Schmidt AD, Strong CDG. Current understanding of epigenetics in atopic dermatitis. Exp Dermatol. 2021;30-45
36. Nicodemus-Johnson J, et al. DNA methylation in lung cells is associated with asthma endotypes and genetic risk. JCI Insight. 2016; 17-25
37. Yang IV, et al. The nasal methylome and childhood atopic asthma. J Allergy Clin Immunol. 2017.119-121
38. Arathimos R, et al. Epigenome-wide association study of asthma and wheeze in childhood and adolescence. Clin Epigenetics. 2017,112-119
39. Bayrak Degirmenci P, et al. Allergic rhinitis and its relationship with IL-10, IL-17, TGF-β, IFN-γ, IL-22, and IL-35. Dis Markers. 2018;258-261
40. Zhou X, Han X, Lyu SC, Bunning BJ, Nadeau KC. Targeted DNA methylation profiling reveals epigenetic signatures in peanut allergy. JCI Insight.
41. 2021;6-14
42. Bilal AA, et al. Histone modifications and their role in epigenetics of atopy and allergic diseases. Allergy Asthma Clin Immunol. 2018;14:39.
43. Kaniskan HU, Martini ML, Jin J. Inhibitors of protein methyltransferases and demethylases. Chem Rev. 2018. 351-360
44. Stefanowicz D, et al. Elevated H3K18 acetylation in airway epithelial cells of asthmatic subjects. Respir Res. 2015;16-95
45. Harb H, et al. Childhood allergic asthma is associated with increased IL-13 and FOXP3 histone acetylation. J Allergy Clin Immunol. 2015 21
46. 35
47. Brook PO, Perry MM, Adcock IM, Durham AL. Epigenome-modifying tools in asthma. Epigenomics. 2015;7:1017-1032.
48. Fujimura KE, et al. Neonatal gut microbiota associates with childhood multisensitized atopy and T cell differentiation. Nat Med.
49. 2016;22:1187-1191.
50. Koizumi SI, Ishikawa H. Transcriptional regulation of differentiation and functions of effector T regulatory cells. 2019;8-15
51. Rachid R, Stephen-Victor E, Chatila TA. The microbial origins of food allergy. J Allergy Clin Immunol. 2021;147:808-813.
52. Wypych TP, et al. Microbial metabolism of l-tyrosine protects against allergic airway inflammation. Nat Immunol. 2021;22 :279-286.

OPEN ACCESS © CINEFORUM